Glass Formation and Shear Elasticity in Dense Suspensions of Repulsive Anisotropic Particles

R. C. Kramb,[1,3] R. Zhang,[2,3] K. S. Schweizer,[1,2,3] and C. F. Zukoski[1,2,3,*]

[1]Department of Chemical and Biomolecular Engineering, University of Illinois, Urbana, Illinois 61801, USA
[2]Department of Materials Science, University of Illinois, Urbana, Illinois 61801, USA
[3]Frederick Seitz Materials Research Laboratory, University of Illinois, Urbana, Illinois 61801, USA

(Received 16 March 2010; published 28 July 2010)

Kinetic vitrification, shear elasticity, and the approach to jamming are investigated for repulsive nonspherical colloids and contrasted with their spherical analog. Particle anisotropy dramatically increases the volume fraction for kinetic arrest. The shear modulus of all systems increases roughly exponentially with volume fraction, and a universal collapse is achieved based on either the dynamic crossover or random close packing volume fraction as the key nondimensionalizing quantity. Quantitative comparisons with recent microscopic theories are performed and good agreement demonstrated.

DOI: 10.1103/PhysRevLett.105.055702 PACS numbers: 64.70.pv, 64.70.Q−, 82.70.Dd, 83.80.Hj

Colloid and nanoparticle science has historically been based on spherical particles that interact via diverse attractive and repulsive forces [1]. Recently, the field has begun to undergo a paradigm shift towards nonspherical and/or chemically heterogeneous (e.g., Janus) particles of modest shape anisotropy [2–4]. A qualitatively new feature is the effect of particle shape on slow dynamics and mechanical properties which is relevant to both dense colloidal suspensions and molecular liquids. Hence, achieving a fundamental understanding of the consequences of breaking particle spherical symmetry is of broad significance in the glass physics field.

Both ideal mode coupling theory (MCT) [5–10] and simulations [11–13] find shape anisotropy deeply modifies kinetic arrest and the glassy shear modulus. For uniaxial hard objects, a remarkable nonmonotonic variation with aspect ratio of the ideal glass transition volume fraction, ϕ_c, is predicted by MCT [5,6] and verified by simulation in a dynamic crossover sense [11]. For symmetric dicolloids composed of two overlapping hard spheres (diameter D) separated by a bond length l_b (sphere center-center separation), ϕ_c is predicted to exhibit a ''maximally fluidic'' state when the aspect ratio $L/D = 1 + (l_b/D) \sim 1.4$ [6,7]. Intriguingly, a similar nonmonotonic variation of the jamming volume fraction of granular ellipsoids and spherocylinders has been discovered [14,15].

Despite significant theoretical progress, systematic experiments that probe the slow dynamics of nonspherical particles which critically test predictions are largely nonexistent. This Letter presents the first quantitative measurements of kinetic arrest and elasticity in suspensions of tunably repulsive nonspherical colloids, and compares the results with their chemically identical spherical analogs. Much prior work has been performed on the latter systems, and many aspects of model hard sphere colloid glassy dynamics are well described by ideal MCT based on continuous cooperative motions [16,17]. Significantly, however, confocal microscopy [18] and simulations [19] find particle trajectories display intermittent large amplitude hopping events, and the MCT nonergodicity transition is avoided due to rare activated processes not captured by ideal MCT. Moreover, recent experiments [20] have established the apparent dominance of activated dynamics above an empirically deduced ϕ_c (larger than the theoretical ϕ_c [19,20]) but well below random close packing (RCP). These latter phenomena are not captured in ideal MCT but are accurately described by the nonlinear Langevin equation (NLE) theory where ergodicity is restored via activated barrier hopping [21] and ϕ_c is a dynamic crossover volume fraction. In this Letter, a kinetic vitrification volume fraction, ϕ_g, is determined as when a relaxation time exceeds a threshold value. New colloidal systems have been designed to test recent theoretical predictions and address four issues: (i) the role of modest shape anisotropy on ϕ_g, (ii) particle shape dependence of the modulus, (iii) possible universality of elasticity, and (iv) possible connection between ϕ_c and ϕ_{RCP}.

Surfactant-based emulsion polymerization methods [22,23] are employed to create four particle shapes: sphere (S) with $D \sim 270 \pm 4$ nm, symmetric homonuclear dicolloid (sDC) of aspect ratio $\sim$1.3 with $D \sim 250 \pm 5$ nm, heteronuclear dicolloid (hDC) of aspect ratio $\sim$1.1 and sphere diameter ratio $\sim$1.2, and a tricolloid (TC) composed of three equal size overlapping spheres of dimensions $D \sim 300 \pm 25$ nm with $l_b \sim 0.45D$. The synthesis is achieved by swelling crosslinked polystyrene seed particles ($D \sim 211 \pm 3$ nm) with additional styrene monomer, and polymerization of added styrene [22]. Phase separation results in the formation of nonspherical particles closely described as overlapping spheres (Fig. 1). We define a characteristic colloid volume V^* as D^3 (S), D^2L (hDC), DL^2 (sDC), and Dbh (TC) where b and h are the base and height of a triangle inscribing the particle.

The physical behaviors of these suspensions are compared at constant chemistry. Interactions were rendered repulsive and short range by stabilizing particles suspended in aqueous electrolytes (NaCl salt) with a monolayer of the nonionic surfactant $C_{12}E_6$ at ionic strengths of

$[I] = 0.03$ M, 0.05 M, and 0.1 M. Classic Derjaguin-Landau-Verwey-Overbeek calculations were performed using a Hamaker constant of 3.1 kT with a minimum polystyrene intersurface separation distance of 8 nm (twice the $C_{12}E_6$ surfactant thickness, 2δ) and electrophoretically derived electrostatic surface potentials [22,23]. The resulting intersphere potentials are shown in Fig. 1. An effective hard diameter, D_{eff} (and corresponding effective volume fraction [24]), is estimated as the distance at which the repulsion is 1 kT. The hard particle model is a good approximation since the total increase in particle diameter is only $\Delta \sim 14.00$ nm at 0.03 M, 11.55 nm at 0.05 M, and 9.85 nm at 0.1 M (where $\Delta \sim 2\delta + \lambda_D$ and λ_D = Debye screening length), and hence the range of the soft electrostatic repulsions is very short ($\Delta/D \ll 1$).

Oscillatory shear mechanical measurements were employed to determine the frequency-dependent elastic (G') and viscous (G'') moduli in the linear response regime. Volume fractions are determined by measuring the mass fraction of polystyrene in a portion of each sample and using reported densities of materials to convert to volume. The experiments are challenging due to limited sample volume and the need to complete measurements before solvent evaporation. In the generalized Maxwell model spirit, a relaxation time,τ, is defined as when $G' = G''$, which correlates closely with other measures of glassy relaxation such as the single particle relaxation time on the cage scale. As illustrated in Fig. 2, a kinetic arrest volume fraction, ϕ_g, is determined based on data at 1 Hz, i.e., $\tau(\phi_g) \equiv 2\pi$ s. Because of experimental uncertainties in measuring ϕ, and the necessity of extrapolating G' and G'' values, ϕ_g is determined to within ± 0.01. The choice of 1 Hz to define kinetic vitrification represents the best compromise between measurement accuracy and the desire to probe low frequencies. We verified for selected systems that the absolute value of ϕ_g is very weakly dependent on this definition, and the reported trends are not tied to using 1 Hz. For example, ϕ_g for the 0.03 M spheres does not change (to 2 significant digits) over the frequency range of 0.1–4 Hz and G' is nearly frequency independent.

Table 1 presents the kinetic glass volume fractions at several ionic strengths. For the most repulsive system ($[I] = 0.03$ M), ϕ_g increases from 0.48 for the sphere to 0.61 for the tricolloid, with the homonuclear and heteronuclear dicolloids in between, thereby showing a large delay of kinetic vitrification from increasing shape anisotropy, qualitatively consistent with theory [5–9]. For fixed particle shape, ϕ_g generally increases with ionic strength, but $[I]$ is a secondary variable that does not modify the overall consequences of nonspherical shape. The main panel of Fig. 2 shows the corresponding dimensionless elastic moduli ($G'^* = G'V^*/\text{kT}$) as a function of ϕ at fixed $[I] = 0.03$ M. The raw data demonstrate kinetic vitrification is strongly particle shape dependent and G' grows roughly exponentially with volume fraction.

How can one understand these observations? The only theoretical approach presently available that has addressed dicolloid and tricolloid shapes, non-hard-core repulsions, and elasticity is the center-of-mass (c.m.) version of "naïve" mode coupling theory (c.m.-NMCT) and barrier hopping NLE theory which are described in detail in the literature [7–9]. Using the known colloid shape and particle interactions, the glassy modulus, ϕ_c, and mean barrier hopping (Kramers) time, τ, can be computed in a first principles manner using the reference interaction site model (RISM) theory [25] of equilibrium correlations as input; all the required equations are in Ref. [7]. Calculations for both the hard core potential and the specific soft repulsions in Fig. 1 have been performed. Physically, the c.m. version of

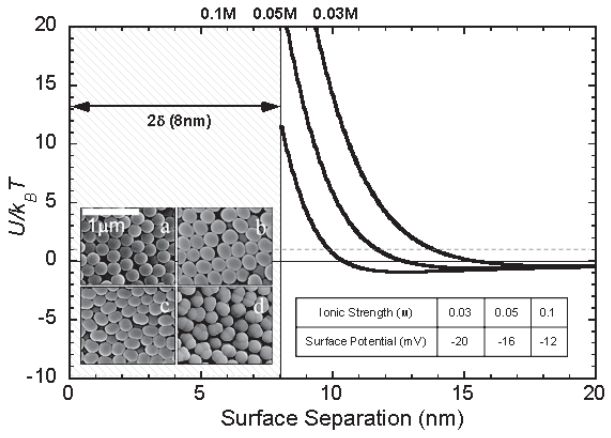

FIG. 1. Pair potentials determined by summation of van der Waals, electrostatic, and surfactant-induced interactions for [I] of 0.03 M, 0.05 M, 0.1 M. The horizontal dashed line is drawn at 1 kT, and defines the distance used for Δ and D_{eff}. (Inset) SEM micrographs of the four particle shapes studied: S (a), hDC (b), sDC (c), and TC (d).

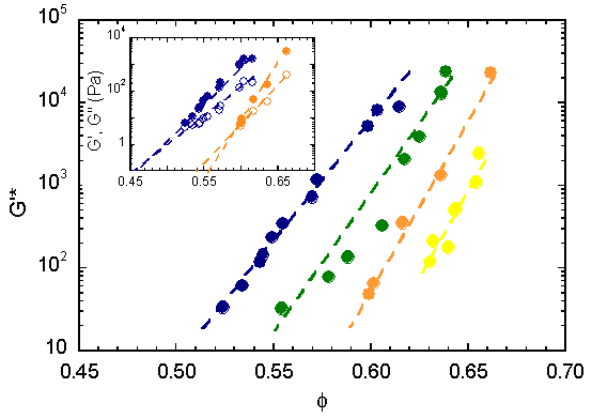

FIG. 2 (color online). Dimensionless elastic modulus, G'^*, as a function of the volume fraction at an ionic strength of 0.03 M [S—blue (darkest), hDC—green (dark grey), sDC—orange (light grey), TC—yellow (lightest)]. (Inset) Method used to determine experimental kinetic glass transition volume fraction. Experimental data for $G'(\phi)$ (closed points) and $G''(\phi)$ (open points) are fit to an exponential and their intersection defines ϕ_g. Data for S and sDC at 0.03 M are shown.

TABLE I. Experimental and theoretical (based on the potentials in Fig. 1) values of the kinetic glass transition volume fraction of the four particle shapes.

Shape	Ionic strength	$\phi_{g(\mathrm{exp})}$	$\phi_{g(\mathrm{theory})}$
S	0.03	0.48	0.545
	0.05	0.48	0.558
	0.1	0.53	0.564
hDC	0.03	0.55	
sDC	0.03	0.59	0.601
	0.05	0.58	0.614
	0.1	0.60	0.618
TC	0.03	0.61	0.645

the NMCT and NLE theory assumes translational motion controls confining force relaxation and cage escape [8]. This simplification (which allows mechanical properties to be determined [7]) is reliable for the modestly anisotropic particles of present interest [10].

c.m.-NMCT calculations yield $\phi_c = 0.432$, 0.474, and 0.508 for the hard core sphere, homonuclear dicolloid, and tricolloid, respectively. This ordering agrees with the experimental kinetic glass transition volume fractions (ϕ_g), but the absolute magnitudes are significantly smaller as expected [21]. The predicted ordering can be physically understood as a consequence of the reduction of all measures of local order at fixed volume fraction as additional single particle length scales enter [7–9]. Weaker dynamical constraints then lead to an increase of ϕ_c in the order S $\rightarrow$ sDC $\rightarrow$ TC.

The main frame of Fig. 3 shows representative NLE theory calculations of τ using the potentials shown in Fig. 1 and the *a priori* computed Brownian short time scale of $\tau_s = 0.1$ sec. A supraexponential increase of τ with volume fraction is evident. Table I presents the theoretical ϕ_g values which follow the same ordering with particle shape as ϕ_c. Good *a priori* (no fitting) agreement with experiment is obtained for the shape and ionic strength dependence trends; quantitatively, the theory overpredicts ϕ_g.

Modulus calculations are presented in the upper inset of Fig. 3 under hard core conditions. As discussed below, the latter potential is used to test the effective hard core model of repulsive particles and because knowledge of the theoretical scaling behavior [7,8] and jamming limit [26] is only available for hard core potentials. Quickly beyond the threshold region, G' increases roughly exponentially with volume fraction over the range studied, and the slopes are weakly sensitive to particle shape, in accord with our experiments. The exponential dependence should be viewed as simply a good approximate representation of the numerical G' calculations. Physically, the ϕ dependence is determined primarily via the increase of local order (and hence dynamical constraints) as volume fraction increases [7]. The lower inset demonstrates G' scales as the inverse localization length squared [7,26], a testable prediction.

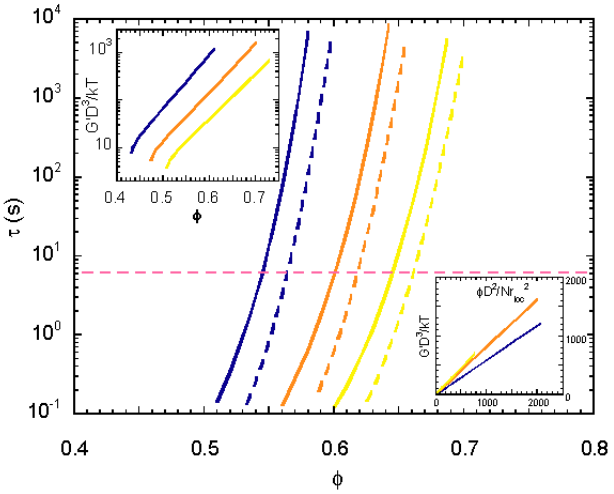

FIG. 3 (color online). Calculated activated relaxation time based on the c.m.-NLE theory [7–9] as a function of volume fraction for S [blue (darkest)], sDC [orange (light grey)], and TC [yellow (lightest)] at ionic strengths of 0.03 M (solid) and 0.1 M (dash). The horizontal line defines kinetic arrest at $\tau = 2\pi$s. (Upper inset) Corresponding modulus calculations under hard core conditions. (Lower inset) Illustration of the generic connection between G' and the inverse localization length squared for the three shapes (N = number of sites per colloid).

Is there an underlying universal behavior of the modulus data in Fig. 2? Prior theoretical work [7,8] for hard core dicolloids suggests the answer is yes if G' is nondimensionalized by V^* defined above, and the distance from the dynamic crossover, $(\phi/\phi_c) - 1$, is adopted as the relevant reduced volume fraction. The theoretical calculations in Fig. 3 are replotted in this doubly reduced fashion in Fig. 4, and an excellent collapse is obtained. Performing the same replotting exercise for the experimental data using ϕ_{eff} [24] also results in a remarkably good collapse as seen in the main frame of Fig. 4 where ϕ_c follows from c.m.-NMCT. Hence, the theoretical suggestion [7,8] that the relevant fundamental stress level involves the single particle volume, and the relevant volume fraction is the distance from the dynamic crossover, is well confirmed. This agreement also supports our proposition that the particles can be modeled as effectively hard. The quantitative difference between theoretical and experiment slopes is not understood, and may reflect quantitative inadequacies of the RISM input.

Now consider the approach to jamming. For hard spheres, it has been analytically predicted [26] $G' \propto g^2(D) \propto (\phi_{\mathrm{RCP}} - \phi)^{-4}$ as RCP is approached. This motivates a double logarithmic plot of the experimental data versus $(\phi_{\mathrm{RCP}} - \phi)^{-1}$. The inset of Fig. 4 presents results for all particle shapes, including the hard sphere data of Ref. [27] for which $\phi_{\mathrm{RCP}} = 0.66$. The RCP volume fraction of nonspherical particles was adjusted to achieve maximum data collapse with the result $\phi_{\mathrm{RCP}} = 0.72$ (dicolloid) and 0.74 (tricolloid). The increase of ϕ_{RCP} with particle asymmetry is physically reasonable. Figure 4

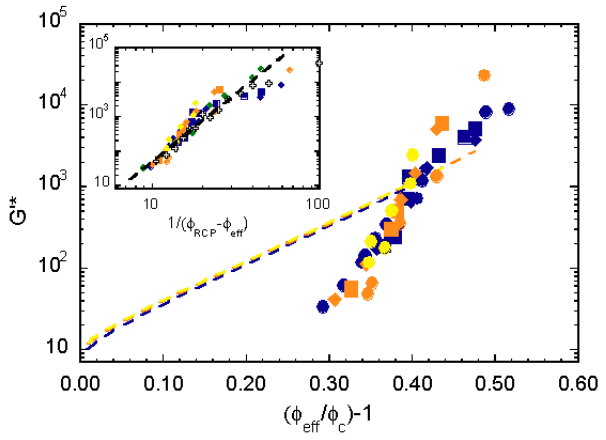

FIG. 4 (color online). Collapse of experimental G'^* data based on the volume fraction scaling $(\phi_{\rm eff}/\phi_c) - 1$, where $\phi_{\rm eff}$ is defined in [24]. Theory (dashed curve) and experimental data (points) are shown for S [blue (darkest)], hDC [green (dark grey)], sDC [orange (light grey)], and TC [yellow (lightest)] and for ionic strengths of 0.03 M (circles), 0.05 M (squares), and 0.1 M (diamonds). (Inset) G'^* plotted as a function of $1/(\phi_{\rm RCP} - \phi_{\rm eff})$. Hard sphere colloid data from Ref. [27] are shown as open points, and a dashed line of slope 4 indicates scaling predicted by theory [26].

shows an excellent data collapse with an effective slope well described by the theory [26].

Interestingly, we have shown above that all the modulus data can be collapsed based on either ϕ_c (dynamic crossover) or $\phi_{\rm RCP}$ (jamming). This suggests a relation exists between the two extreme limits of this glass physics problem. Using the experimentally deduced $\phi_{\rm RCP}$ and the c.m.-NMCT value for ϕ_c, we find their ratio is nearly constant: $\phi_{\rm RCP}/\phi_c : 1.50 \pm 0.04$. This provides additional support for a connection between the onset of activated dynamics and granular jamming. The G' calculations have also been analyzed in the above fashion, and a good collapse is obtained (not shown) with best fit values: $\phi_{\rm RCP} =$ 0.66 (sphere), 0.72 (dicolloid), 0.76 (tricolloid), close to those deduced from the experimental data collapse. We note that prior ideal MCT studies of binary hard sphere mixtures [28] and hard nonspherical particle systems [7,13] also found a close connection between ϕ_c and $\phi_{\rm RCP}$.

In conclusion, we have performed the first combined experimental-theoretical study of kinetic vitrification and elasticity in dense suspensions of repulsive nonspherical colloids. Modest shape anisotropy strongly delays kinetic arrest. The modulus grows roughly exponentially with volume fraction, and a theoretically inspired universal master plot can be achieved for all shapes and repulsion strengths based on either the ideal MCT crossover or RCP jamming as the relevant measure of crowding. Our observations are in good accord with theoretical ideas.

Our work is supported by the U.S. Department of Energy under Grant No. DE-FG02-07ER46471, through the Frederick Seitz Materials Research Laboratory (FS-MRL) at Illinois. Experiments were carried out in part in the FS-MRL Central Facilities, which are partially supported by Grants No. DE-FG02-07ER46453 and No. DE-FG02-07ER46471.

*czukoski@illinois.edu, kschweiz@illinois.edu

[1] W. B. Russel, D. A. Saville, and W. R. Schowalter, *Colloidal Dispersions* (Cambridge University Press, Cambridge, England, 1989).
[2] S. C. Glotzer and M. J. Solomon, Nature Mater. **6**, 557 (2007).
[3] A. van Blaaderen, Nature (London) **439**, 545 (2006).
[4] S. Jiang *et al.*, Adv. Mater. **22**, 1060 (2010).
[5] M. Letz, R. Schilling, and A. Latz, Phys. Rev. E **62**, 5173 (2000).
[6] S.-H. Chong and W. Götze, Phys. Rev. E **65**, 041503 (2002).
[7] G. Yatsenko and K. S. Schweizer, J. Chem. Phys. **126**, 014 505 (2007).
[8] G. Yatsenko and K. S. Schweizer, Phys. Rev. E **76**, 041506 (2007).
[9] M. Tripathy and K. S. Schweizer, J. Chem. Phys. **130**, 244 906 (2009).
[10] R. Zhang and K. S. Schweizer, Phys. Rev. E **80**, 011502 (2009).
[11] A. J. Moreno *et al.*, J. Chem. Phys. **123**, 204 505 (2005).
[12] C. De Michele, R. Schilling, and F. Sciortino, Phys. Rev. Lett. **98**, 265702 (2007).
[13] P. Pfleiderer, K. Milinkovic, and T. Schilling, Europhys. Lett. **84**, 16 003 (2008).
[14] A. Donev *et al.*, Science **303**, 990 (2004).
[15] S. Sacanna *et al.*, J. Phys. Condens. Matter **19**, 376 108 (2007).
[16] W. Götze and L. Sjörgen, Rep. Prog. Phys. **55**, 241 (1992).
[17] W. van Megen and S. M. Underwood, Phys. Rev. E **49**, 4206 (1994).
[18] E. R. Weeks and D. A. Weitz, Chem. Phys. **284**, 361 (2002).
[19] S. K. Kumar, G. Szamel, and J. F. Douglas, J. Chem. Phys. **124**, 214 501 (2006); Y. Brumer and D. R. Reichman, Phys. Rev. E **69**, 041202 (2004).
[20] G. Brambilla *et al.*, Phys. Rev. Lett. **102**, 085703 (2009).
[21] K. S. Schweizer and E. J. Saltzman, J. Chem. Phys. **119**, 1181 (2003); K. S. Schweizer, Curr. Opin. Colloid Interface Sci. **12**, 297 (2007).
[22] E. B. Mock *et al.*, Langmuir **22**, 4037 (2006); R. C. Kramb and C. F. Zukoski, *ibid.* **24**, 7565 (2008).
[23] S. J. Partridge, Ph.D. thesis, Bristol University, 1985.
[24] The effective hard core volume fraction is defined as $\phi_{\rm eff} = \phi(V^*_{\rm eff}/V^*)$, where V^* is defined in the text and all effective lengths are larger by an amount Δ.
[25] D. Chandler and H. C. Andersen, J. Chem. Phys. **57**, 1930 (1972).
[26] K. S. Schweizer and G. Yatsenko, J. Chem. Phys. **127**, 164 505 (2007).
[27] N. Koumakis, A. B. Schofield, and G. Petekidis, Soft Matter **4**, 2008 (2008).
[28] W. Gotze and T. Voigtmann, Phys. Rev. E **67**, 021502 (2003); D. Hajnal, J. M. Brader, and R. Schilling, Phys. Rev. E **80**, 021503 (2009).